SEISMIC PERFORMANCE EVALUATION
OF JAPANESE WOODEN FRAMES

Masumi YAMADA[1], Yoshiyuki SUZUKI [2], and Masami GOTOU[3]

SUMMARY

Shaking table tests were carried out for wooden frames with three different seismic resistant elements respectively, as well as the same frame without any additional structural elements. The structural elements are plaster walls used in traditional wooden houses, and wooden braces and plywood walls used in modern wooden houses. Hysteretic behaviors of these frames are investigated based on the test results.

Important characteristics of the hysteretic behaviors, which are critical for the seismic performance, are discovered and compared between the four frames. Constitutive models are proposed to represent hysteretic restoring forces analytically using the test results, and apply to the different frames for simulating their dynamic behaviors. It is found both experimentally and analytically that, among the four frames, the traditional wooden frame with plaster walls has both a large maximum restoring force and a high deformability; therefore, it has the best seismic performance.

INTRODUCTION

Traditional Japanese wooden buildings are typically composed of wooden frames with mortise and tenon connections, as well as plaster walls to enclose the buildings and separate rooms. In modern wooden houses, plaster walls have been widely used to replace the plaster walls for construction convenience, and wooden braces have been added to strengthen the structures. The walls and braces in fact play important roles in resisting earthquakes. Unfortunately, structural analyses of wooden buildings are difficult because of inhomogeneities and unpredictable behaviors of timber and the complexity and variation in construction methods. Consequently, their seismic performances have yet to be fully evaluated although pioneer works have begun recently by Sakamoto et. al. [1], Suzuki and Nakaji [2] and Yamaguchi et. al. [3].

In order to investigate seismic performances of wooden frames with various structural elements, shaking table tests were carried out in the Disaster Prevention Research Institute (DPRI), Kyoto University [4,5]. Test specimens included a basic wooden frame and three frames by adding traditional

---

[1] California Institute of Technology, M. Eng. masumi@caltech.edu

[2] Prof., Disaster Prevention Research Institute, Kyoto University, Dr. Eng. suzuki@zeisei.dpri.kyoto-u.ac.jp

[3] Associate Prof., Department of Engineering, Kanazawa Institute of Technology, Dr. Eng.
gotou@neptune.kanazawa-it.ac.jp

plaster walls, wooden braces, and plywood walls respectively. The excitation intensity was being increased gradually until destructions took place. Hysteretic behaviors of the specimens were investigated, different failure modes were observed for the specimens, and seismic performances of the different seismic resistant elements were evaluated and compared.

Using the test results, an analytical method is proposed to model the hysteresis of wooden frames. The established analytical hysteresis models for the four specimens are then used for a dynamic analysis under different roof weights, and their seismic performances are evaluated.

SHAKE TABLE TESTS OF WOODEN FRAMES

Test Specimens

The basic specimen was composed of two planar frames connected to each other by a horizontal wooden roof shown in Figures 1 and 2(a). Each frame consisted of a pair of columns and two beams connecting them at the base level and the roof level, respectively, by using stud tenons with nail plates. The sizes of these components are shown in Figure 2(a). The basic specimen will be called frame only specimen in this paper.

Various types of seismic elements were incorporated in the frames, including traditional plaster walls, wooden braces, and plywood walls. Only one type of elements was installed in a basic frame specimen so that seismic performances could be evaluated respectively for each type.

The plaster-wall specimen was constructed by adding three tie-beams and one supporting beams in a basic frame, forming a lattice of tied bamboo, and covering it with three layers of coarse sand, fine sand, and lime plaster from inside to outside, as shown in Figure 2(b) and Photo 1.

Figure 1 : Specimen

The total thickness of the wall was 60mm. The plaster walls have been built in traditional wooden houses. They are typical shear walls from structural point of view. In the wooden-brace specimen, a supporting column and two diagonal wooden braces were added, as shown in Figure 2(c). The braces were fastened to the column-beam joints with corner plates. The plywood-wall specimen, shown in Figure 2(d), was constructed by adding three supporting columns and three plywood panels. The plywood panels were fastened to the frame by nails with a uniform spacing of 150mm. The plywood panels were commercially available. The sizes of these components are shown in Figures 2(a) through 2(d).
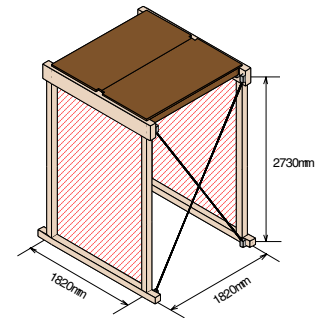
Shaking and Measurement Method

The shaking table tests, as shown in Photo 2, were performed using a strong earthquake response simulator in DPRI, Kyoto University. Steel plates of different weights were attached to the roofs of the different specimens, respectively, so that the natural period of each specimen was normalized to 1 second. The weights are shown in Table 1. Input seismic wave was the "building center of Japan level 2 seismic wave" (BCJ-L2). Figures 3(a) and 3(b) show the time history and the velocity response spectrum of the BCJ-L2 wave, respectively. Each specimen was excited repeatedly with an increasing intensity of scaled BCJ-L2 waves until a critical damage occurred. The maximum acceleration of a scaled BCJ-L2 wave is used as the specification for the excitation intensity level in the paper. The shaking table was excited only in the horizontal direction parallel to the frame plane.

Accelerometers were installed on the roofs of the specimens, and the measured accelerations were used to calculate the restoring forces of the specimens. Displacements were measured by laser displacement sensors attached at the ends of the roof beams and base beams. Deformation angles were obtained from the interstory drifts and the height of the specimens. Strain gauges were mounted on both ends of columns, braces, and penetrating tie beams to obtain stresses at these locations.
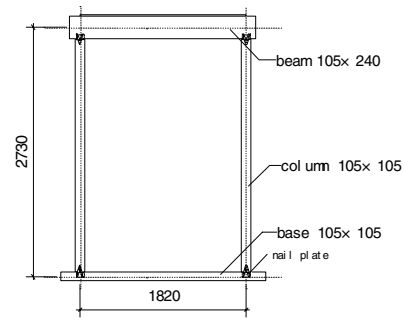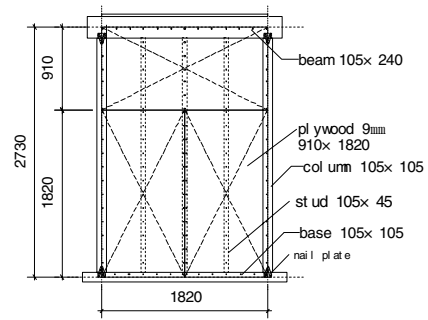
(a) Frame-only specimen
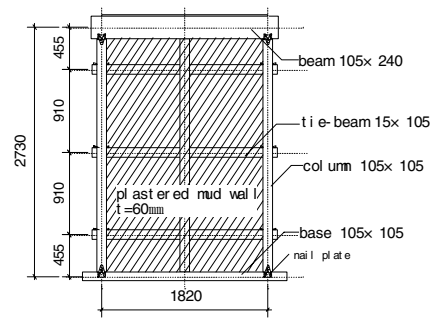
(b) Plaster-wall specimen
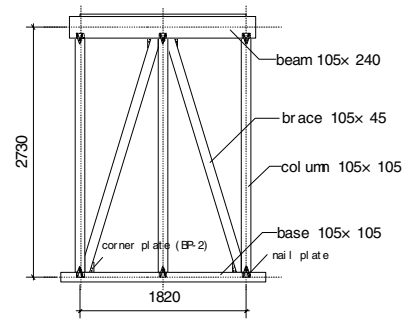
(c) Wooden-brace specimen

(d) Plywood-wall specimen

Figure 2 : Elevations of specimens (All dimensions in mm.)

Photo 1: Plastering the test specimen.

Photo 2: Specimen ready for testing.

Table 1 : List of specimens

Test specimen	Seismic resisting elements	Weight (kN)	
		Total weight	Specimen only
frame only	simple frame without wall	4.9	1.6
with plywood-walls	9mm structural plywood	39.2	1.9
with wooden-braces	two diagonal wooden braces (105*45 mm)	29.4	1.8
with plaster-walls	60mm mud plaster wall	39.2	4.7

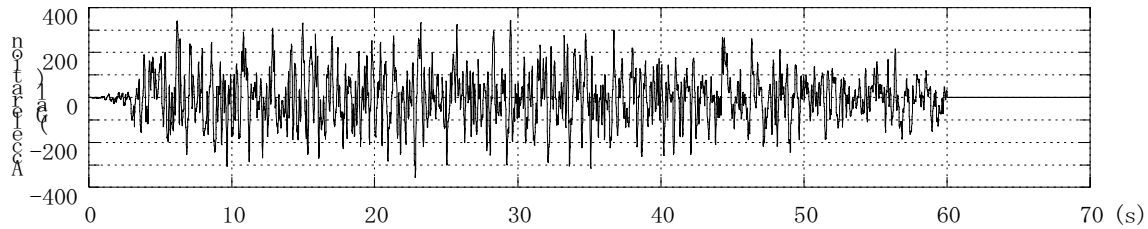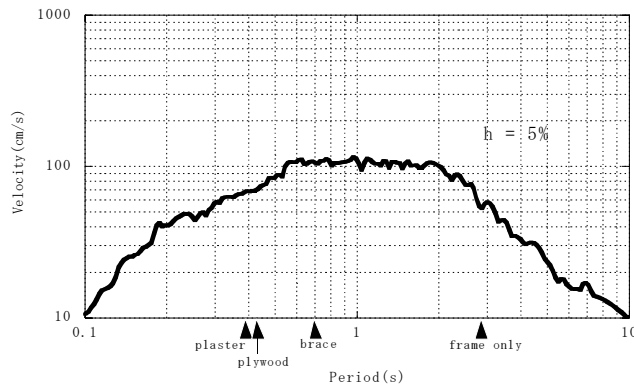Figure 3(a) : Time history of BCJ-L2

Figure 3(b) : Velocity response spectrum of BCJ-L2

TESTS RESULTS

Restoring Force and Failure of Specimens

Figures 4(a) through 4(d) show the restoring force characteristics of the four test specimens, respectively. The thick solid line in each figure represents the backbone curve of the restoring force for the test specimen. It was obtained by increasing the excitation level gradually until damages took place. A point on the backbone curve represents the maximum force and the corresponding deformation angle at a certain level of the excitation. The thin-line loops in each figure describe hysteretic characteristics of the specimen at an excitation level specified in the figure. For comparison, the backbone curve of the frame only specimen is added to Figures 4(b) through 4(c) by thick dashed lines.

In the tests on the plaster-wall specimen, a crack was observed (see Photo 3) when the deformation angle reached 0.005rad. But this minor damage had little effect on the entire structure strength. The restoring force continued to increase until the deformation angle reached 0.025rad, when

corners of the plaster walls started to crumble (see Photo 4). At this angle, the restoring force reached its maximum value close to 16kN. We define this angle as the critical deformation angle of the specimen. The importance of this angle will be described in the next section. As the deformation increased, corners of the plaster walls crumbled further, and out-of-plane buckling took place (see Photo 5), resulting in a sharp decrease of the restoring force.

The tests on the wooden-brace specimen stopped at the deformation angle of 0.04rad when a wooden brace broke (see Photo 6). The restoring force was 8.4kN at this point.

In the tests on the plywood-wall specimen, nails at corners of the plywood panels started to be pulled out at the angle of 0.014rad, at which the restoring force reached its maximum of 12.5kN. Immediately after it, out-of-plane buckling occurred (see Photo 7). The pullout of the nails caused the separation of the plywood panels from the frame, resulting in a sudden drop in the restoring force.

Comparing the four specimens, it is found that the maximum restoring forces of the three specimens with the seismic resistant elements were much higher that that of the frame only specimen. It was about 16kN for the plaster-wall specimen, 12.5kN for the plywood-wall specimen, 8.4kN for the wooden-brace specimen, and 1.2kN for the frame only specimen.
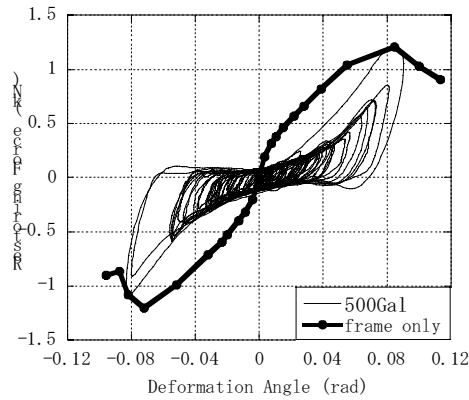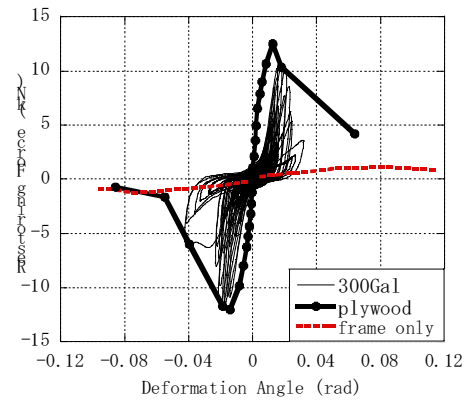

(a) Frame-only specimen
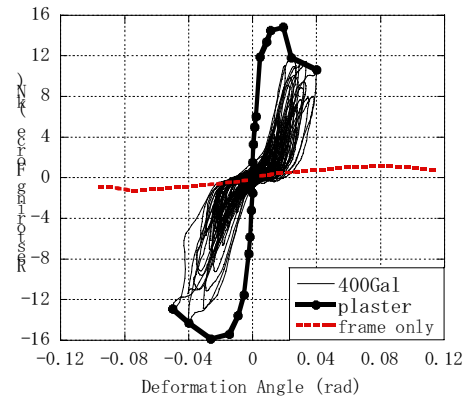
(b) Plaster-wall specimen
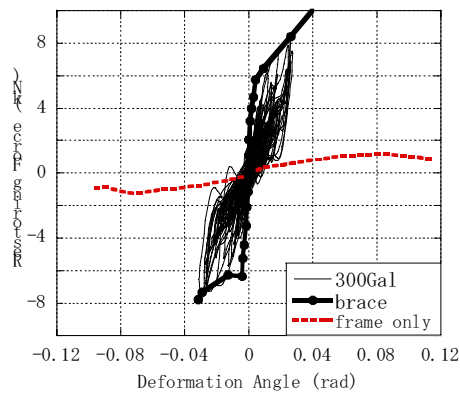
(c) Wooden-brace specimen

(d) Plywood-wall specimen

Figure 4 : Restoring force characteristics

Photo 3 : [Plaster-wall test] Crack on a plaster surface.

Photo 4 : [Plaster-wall test] Crumbling of a corner of a plaster wall.
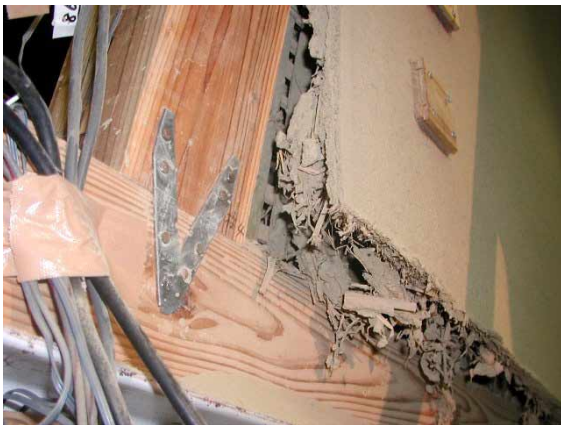

Photo 5 : [Plaster-wall test] Out-of-plane buckling of a plaster wall.

Photo 6 : [Wooden-brace test] Broken wooden brace.

Photo 7 : [Plywood-wall test] Out-of-plane buckling of a plywood panel.

Photo 8 : [Plywood-wall test] Deterioration at corners of plywood panels.

Deformability

It is known that traditional wooden houses are capable of undergoing large deformations. The term deformability is usually used to describe the capacity of a structure to maintain structural integrity under large deformations. Since the deformation is the main cause for structure damages, the deformability is one of the most important characteristics of structure seismic resistance.

Figure 5 depicts four backbone curves of the restoring forces for four specimens, with the restoring forces normalized by their respective maximum values. The critical deformation angle was 0.085rad for the frame only specimen, 0.025rad for the plaster-wall specimen, 0.04rad for the wooden-brace specimen, and 0.014 for the plywood-wall specimen. After the critical deformation angle, the restoring force of the plywood-wall specimen dropped rapidly due to the onset of brittle out-of-plane buckling. Data for the wooden-brace specimen after the brace fracture was not obtained, but results from past experiments indicated that the restoring force would drop rapidly [6]. In contrast to these two specimens, the restoring force of the plaster-wall specimen decreased gradually after the maximum value was reached, and the specimen retained a high level of the restoring force in a considerably large deformation range. Similar phenomenon was also observed for the frame only specimen.

Two features in a backbone curve of the restoring force determine the deformability of a structure. One is the angle at the peak point, namely the critical deformation angle. Before this point, the structure restoring force is increasing and the structure maintains its integrity. Thus a large critical deformation angle indicates a larger allowable deformation. The second feature is the behavior of the restoring force after the peak point. A sharp drop in the restoring force points out that the structure has lost its seismic resistance quickly, and severe damages have taken place in the structure. In this case, the critical deformation angle gives the maximum allowable deformation. On the other hand, a gradual reduction in the restoring force indicates that no severe damages have occurred immediately and the structure still keeps its major seismic resistance although it becomes more vulnerable. Thus, the maximum allowable deformation can be larger that the critical deformation angle to an extent depending on the risk tolerance. Comparing the four backbone curves, it is found that both the frame only specimen and the plaster-wall specimen possess large deformability. Results of static loading tests on the same plaster-wall specimen also showed that its restoring force kept more then 1/3 of the maximum restoring force even when the deformation angle reaches 0.09rad [7].

In conclusion, the frame only specimen does not provide a large restoring force although it had a high deformability, and only the plaster-wall specimen has both a large maximum restoring force and a high deformability. This result is consistent with earthquake damage surveys that showed many traditional wooden houses with plaster walls did not collapse even having experienced large deformation (more than 0.01rad) [8].
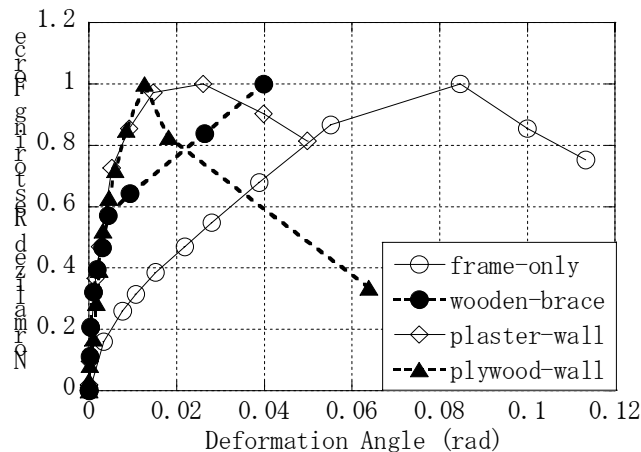

Figure 5 : Comparison of backbone curves.

HYSTERESIS MODELLING OF WOODEN FRAMES

Modeling of the hysteresis loops

Hysteresis loops for a wooden frame are dependent on the excitation level. The characteristics are governed by the frame structure, properties of structural materials, joint structures, etc. [9]. Figure 6 shows the hysteresis loops of the frame only specimen at an excitation level 500Gal, obtained from the shaking table tests. Several typical features of the wooden frame hysteresis can be observed from the figure. The force-deformation relationship is nonlinear and there is no distinct yield point. After the restoring force reaches the maximum value in a loop, two stages, unloading and slipping stage, follow, as shown in Figure 6. During unloading stage, the stiffness, i.e. the slope of the curve, is quite high. Although it changes with the deformation, the variation is not large. It is found that the stiffness in this stage is approximately equal to the initial stiffness. Thus, the initial stiffness can be used for the unloading stiffness. The slipping is referred to the phenomena that the deformation changes without requiring much change in loading. Thus, in the slipping stage, the stiffness is very small, even zero or negative. It can be seen from Figure 6 that no slipping appears if the deformation is small. It takes place when the deformation is larger, and the slipping stage becomes longer with an increasing deformation. The slipping stiffness is varying during the slipping stage.

In order to carry out various analyses for wooden frames, an analytical model is desired for describing their hysteretic behaviors quantitatively. Taking the above described hysteresis features in consideration, three models using piecewise linear functions and possessing the same backbone curve are proposed. They are shown in Figures 7(a) through 7(c), and described below.

[a] Degrading Bi-linear Model (DBL Model)

DBL model is illustrated in Figure 7(a) where points P_2 and P_3 are fixed and determined from the hysteresis loops obtaining from tests, and P_0 is a point on the backbone, i.e. the point at which the maximum deformation is reached in a hysteresis loop. The loading stage is from P_3 to P_0. In the unloading stage ($P_0 \rightarrow P_1$), the stiffness is the same as the initial stiffness. Modified from the bi-linear model, DBL model includes a slipping stage ($P_1 \rightarrow P_2$) with stiffness equal to the slope of line P_0-P_3. This model describes the hysteretic behavior when the maximum deformation of a loop is small.

[b] Original Degrading Bi-linear Model (ODB Model)

This is a bi-linear model with a zero slipping stiffness, as shown in Figure 7(b). The loading process is the same as that of DBL model, and the initial stiffness is employed in the unloading stage ($P_0 \rightarrow P1$). The slipping stage passes point P_2. By combining ODB and DBL models, the slipping stiffness can be controlled based on the maximum deformation of a loop.

[c] Original Slip Model (OSL Model)

This is a slip model shown in Figure 7(c). In the loading stage, it slips on the X-axis from the origin to P_3, at which point a half of the maximum deformation is reached. Then it heads to P_0. The slipping stage during the unloading is also on X-axis.

These three models are combined to represent the hysteresis of a wooden frame. The model parameters, such as the initial stiffness, the backbone curve, the location of P2 and P3, as well as the weights distributed to each model are determined by the test results. Figure 8 shows the weight distribution for the frame only specimen. When the deformation angle is less than 0.01rad, the hysteresis loops behave sorely as the DBL model. As the deformation angle increasing, the stiffness in the slipping stage decreases, and ODB and/or OSL models are added to the model. Only ODB model is added if the angle is between 0.01 and 0.03rad, and the weight assigned to each model can be determined from Figure 8. All three models are used at the angle range of 0.03-0.05rad, and only ODB and OSL models are used with an equal 50% weight when the angle exceeds 0.05rad. Note that the sum of all weights distributed to

different models should be one so that the analytical model has the same backbone as that obtained from tests.

Using the three models, analytical hysteresis models have been established for the four specimens, respectively, based on the test results shown in Figures 4 and 5. To substantiate the models, dynamic analyses were conducted to the specimens. Each original frame was replaced by an equivalent single-degree-of-freedom (SDOF) system with the same mass and the analytical hysteretic restoring force. Numerical calculations were carried out to obtain responses of the equivalent SDOF systems. Figures 9 and 10 show the test results and analytical results for the frame only specimen under the excitation of BCJ-L2 500Gal. The basic features of the hysteresis loops, such as the loop shapes, loop areas, the maximum restoring force, the maximum deformation angle, etc., agree quite well between the two results. Comparisons were also made for the three specimens with structural elements, and similar conclusions could be drawn.
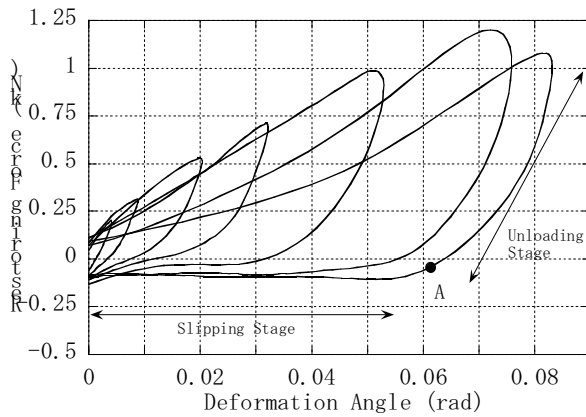
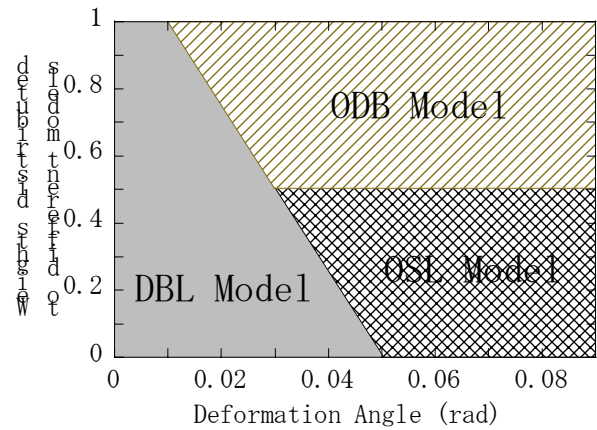Figure 6 : Hysteresis loops of the frame-only specimen
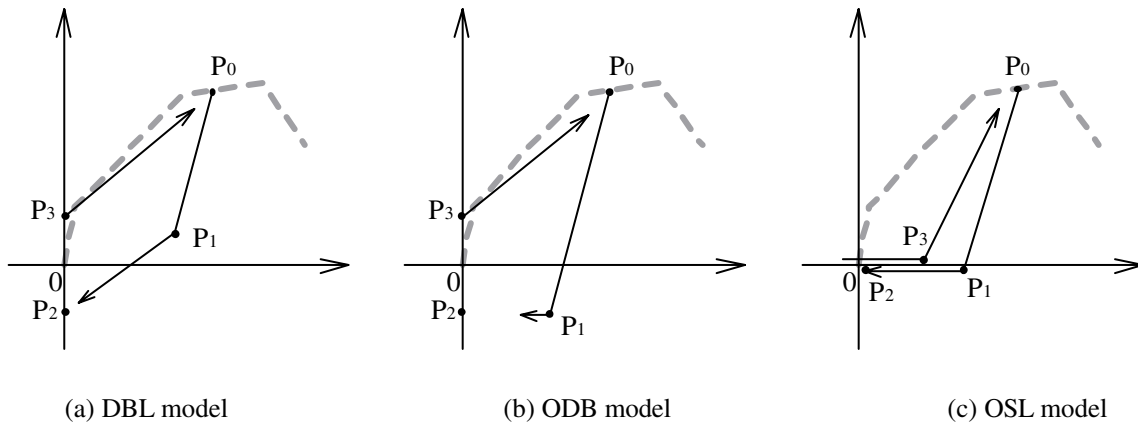
Figure 8 : Combination of the models

(a) DBL model

(b) ODB model
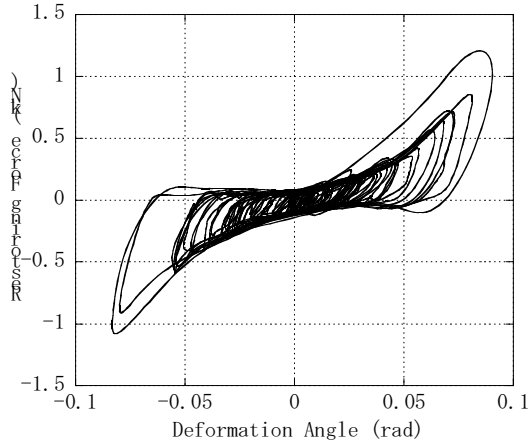
(c) OSL model

Figure 7 : The hysteresis models

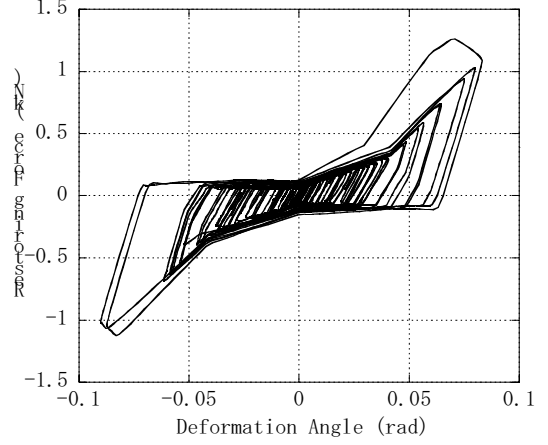Figure 9 : Experimental results for frame-only specimen

Figure 10 : Analytical results for frame-only specimen

Dynamic analysis

The analytical models for the four specimens can now be used for dynamic analyses to evaluate seismic performances. It is found from tests that the weight added on the roof of a frame does not have significant effect on the hysteretic behavior of the frame. Thus, we can use the analytical models to estimate effects of the roof weight on the seismic performance. As an example, two different values of 1000kg and 2000kg are assigned to the weight of each equivalent SDOF system for the specimens   This is equivalent to add different weights on the roofs of the different specimens. The same excitation of BCJ-L2 350Gal is applied, and the P-d effect is neglected in all cases

Figure 11 shows the analytical results for the four specimens with an equal weight of 9.8kN. The deformation of the frame only specimen exceeds 0.05rad, while those of the other specimens are less than 0.01rad. Under the same level of excitation, the plaster-wall specimen has the highest stiffness and the smallest deformation angle. The same dynamic analysis is performed for the case of 19.6kN weight, and the results are shown in Figure 12. Brittle fractures can be seen for the wooden-brace specimen and the plywood-wall specimen as the restoring forces drop rapidly as the deformations reach certain critical values. The maximum deformation angle of the plywood-wall specimen is over 0.08rad, while the deformation angle of the plaster-wall specimen remains less than 0.01rad even though the mass is doubled.

The above analyses show the brittle fracture phenomena occurring in both the wooden-brace specimen and the plywood-wall specimen, and show the highest seismic performance of the plaster-wall specimen among the underlying four specimens.
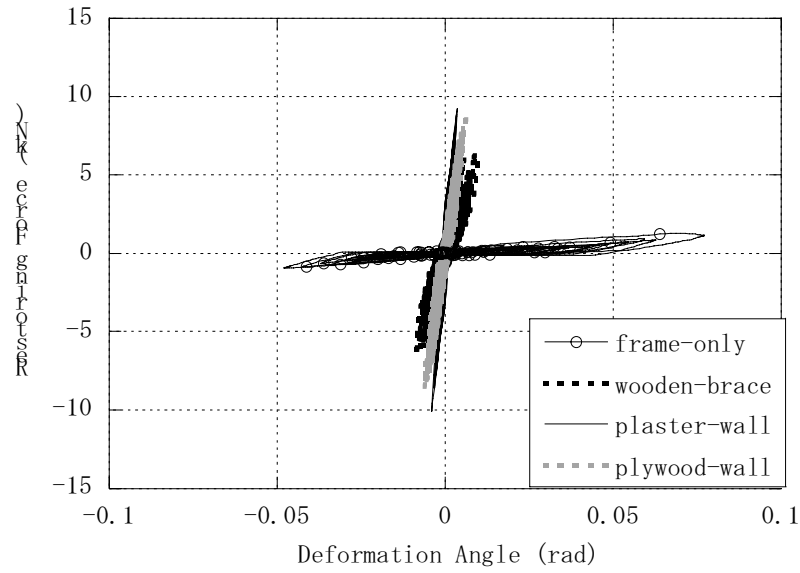
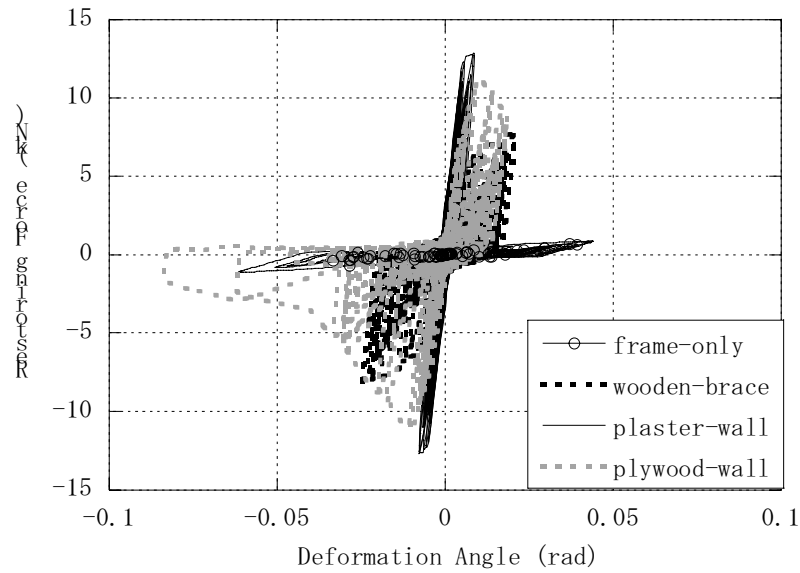Figure 11 : Dynamic analysis of four specimens (mass=1000kg)

Figure 12: Dynamic analysis of four specimens (mass=2000kg)

CONCLUSION

The results obtained from the shaking table tests on the wooden frames show that the location and behavior at the peak point on the backbone curve are critical for the seismic performance of a wooden structure. At the peak point, the restoring force reaches its maximum value, which is an indication of the seismic resistant ability. The deformation angle at the peak point, namely the critical deformation angle, gives a safe range for the deformation; thus, it is the most explicit sign of the deformability. And the behavior after the peak point reflects if the structure is brittle or flexible, which is also an important aspect

of the deformability. The test results show that the plaster-wall specimen has a high restoring force, a large critical deformation angle, and flexible characteristic at the peak point; therefore, it is the best among the three seismic resistant elements.

An analytical method to model the hysteresis of a wooden frame is proposed. Although test data are needed in the modeling, an established analytical model is able to represent the restoring force of the structure, and can be used for various dynamic analyses. The analysis using the proposed modeling method also shows that the plaster-wall frame has the best seismic performance.

REFERENCES

[1] Sakamoto I., Ohashi Y., Fujita K., et al. (1997). "Shaking Table Test of Kumimono used in Traditional Wooden Structure (Part1, 2). " Proceedings of Kanto Branch, Architectural Institute of Japan, pp.37-44, 1997. (in Japanese)

[2] Suzuki Y. and Nakaji H. (1999). "Reexamination of Seismic Resistance of Mud-plastered Walls in Wood Houses Based on Full-scale Tests." Journal of Structural and Construction Engineering, No.515, pp.115-122, Jan. 1999. (in Japanese)

[3] Yamaguchi N., Karacabeyli E., Minowa C., Kawai N., Watanabe K. and Nakamura I. (2000). "Seismic Performance of Nailed Wood-frame Shear Walls." World Conference on Timber Engineering, Sec. 8.1.1, July 2000.

[4] Suzuki Y., Goto M. and Yamada M. (2002). "Evaluation of Seismic Performance of Wooden Frames by Shaking Table Tests." The 11th Japan Earthquake Engineering Symposium, pp.1511-1516, 2002.11. (in Japanese)

[5] Goto M., Yamada M. and Suzuki Y. (2002). "Dynamic and Static Tests of Wooden Frames for Evaluation of Seismic Performance." The 11th Japan Earthquake Engineering Symposium, pp.1517-1522, 2002.11. (in Japanese)

[6] Nakaji H. (1999). "Evaluation of Seismic Performance for Wooden Structures." PhD thesis, Kyoto University, Kyoto, Japan, pp.49-57, April 1994. (in Japanese)

[7] Yamada M., Suzuki Y., Gotou M. and Shimizu H. (2003). "Dynamic and Static Tests of Wooden Frames for Evaluation of Seismic Performance." Journal of Structural and Construction Engineering (under review).

[8] Kitahara A., Hayashi Y., Okuda T., Suzuki Y. and Goto M (2002). "Structural Characteristics and Earthquake Damage of Wooden Houses in the 2000 Western Tottori Earthquake." Journal of Structural and Construction Engineering, No.561, pp.161-167, Nov. 2002. (in Japanese)

[9] Foliente G. C. (1995). "Hysteresis Modeling of Wood Joints and Structural Systems." Journal of Structural Engineering, pp.1013-1022, June 1995.

ACKNOWLEDGEMENTS